Langmuir
The ACS Journal of Surfaces and Colloids

JULY 4, 2006
VOLUME 22, NUMBER 14

Letters

Nanoscale Surface Patterns from 10_3 Single Molecule Helices of Biodegradable Poly(L-lactic acid)

Suolong Ni,[†] Wen Yin,[†] Melinda K. Ferguson-McPherson,[†] Sushil K. Satija,[‡] John R. Morris,[†] and Alan R. Esker*,[†]

Department of Chemistry (0212), Virginia Polytechnic Institute and State University, Blacksburg, Virginia 24061, and Center for Neutron Research, National Institute of Standards and Technology, Gaithersburg, Maryland 20899

Received March 18, 2006. In Final Form: May 4, 2006

Atomic force microscopy, reflection absorption infrared spectroscopy, and X-ray reflectivity studies reveal that poly(L-lactic acid) molecules in Langmuir−Blodgett (LB) films exist as 10_3 helices over nearly the entire length of the polymer chain. This feature gives rise to LB films with highly ordered nanoscale smectic liquid crystalline-like surface patterns with low surface roughness and lamellar spacings that scale with molar mass. These studies provide a new approach for controlling surface morphology with a biodegradable polymer commonly used for drug delivery and tissue engineering.

Introduction

Nanometer-scale pattern formation via the organization of molecules is a key challenge in nanoscale science and technology.[1] Recently, there is an increasing interest in fabricating a surface with a polymer layer, which can dramatically alter the properties of the surface for applications in adhesion, drug delivery, data storage, etc.[2−4] Various techniques have been used to fabricate nanopatterns with polymers onto solid surfaces, including soft lithography, nanoimprinting lithography, dip-pen nanolithography, polymer spin transfer printing, laser stereolithography, nanosphere lithography, the Langmuir−Blodgett (LB) technique, etc.[5−9] Among these techniques, the LB technique facilitates the fabrication of highly ordered films with monolayer by monolayer control of thickness and low surface roughness.[10−13] The LB technique has been applied to prepare surface patterns using block copolymers[14] and phopholipids,[15] thereby providing control over surface structures and properties, which is desirable for a number of applications such as cell adhesion.[16]

Controlling surface morphology with a biodegradable and biocompatible synthetic polymer, poly(lactic acid) (PLA), has attracted considerable interest because of its importance in tissue

* To whom correspondence should be addressed. E-mail: aesker@vt.edu. Fax: (01) 540-231-3255.
[†] Virginia Polytechnic Institute and State University.
[‡] National Institute of Standards and Technology.

(1) Geissler, M.; Xia, Y. N. *Adv. Mater.* **2004**, *16*, 1249−1269.
(2) Sigal, G. B.; Mammen, M.; Dahmann, G.; Whitesides, G. M. *J. Am. Chem. Soc.* **1996**, *118*, 3789−3800.
(3) Santini, J. T.; Richards, A. C.; Scheidt, R.; Cima, M. J.; Langer, R. *Angew. Chem., Int. Ed.* **2000**, *39*, 2397−2407.
(4) Prime, K. L.; Whitesides, G. M. *Science* **1991**, *252*, 1164−1167.
(5) Xia, Y. N.; Whitesides, G. M. *Annu. Rev. Mater. Sci.* **1998**, *28*, 153−184.
(6) McAlpine, M. C.; Friedman, R. S.; Lieber, C. M. *Nano Lett.* **2003**, *3*, 443−445.
(7) Matsuda, T.; Mizutani, M.; Arnold, S. C. *Macromolecules* **2000**, *33*, 795−800.
(8) Lu, Y.; Chen, S. C. *Nanotechnology* **2003**, *14*, 505−508.
(9) Park, J.; Kim, Y. S.; Hammond, P. T. *Nano Lett.* **2005**, *5*, 1347−1350.
(10) Petty, M. C. *Langmuir−Blodgett Films: An Introduction*; Cambridge University Press: Cambridge, 1996.
(11) Sackmann, E. *Science* **1996**, *271*, 43−48.
(12) Esker, A. R.; Mengel, C.; Wegner, G. *Science* **1998**, *280*, 892−895.
(13) Zasadzinski, J. A.; Viswanathan, R.; Madsen, L.; Garnaes, J.; Schwartz, D. K. *Science* **1994**, *263*, 1726−1733.
(14) Li, S.; Clarke, C. J.; Lennox, R. B.; Eisenberg, A. *Colloids Surf., A* **1998**, *133*, 191−203.
(15) Moraille, P.; Badia, A. *Angew. Chem., Int. Ed.* **2002**, *41*, 4303−4306.
(16) Sivasankar, S.; Brieher, W.; Lavrik, N.; Gumbiner, B.; Leckband, D. *Proc. Natl. Acad. Sci. U.S.A.* **1999**, *96*, 11820−11824.

10.1021/la060734a CCC: $33.50
Published on Web 06/03/2006

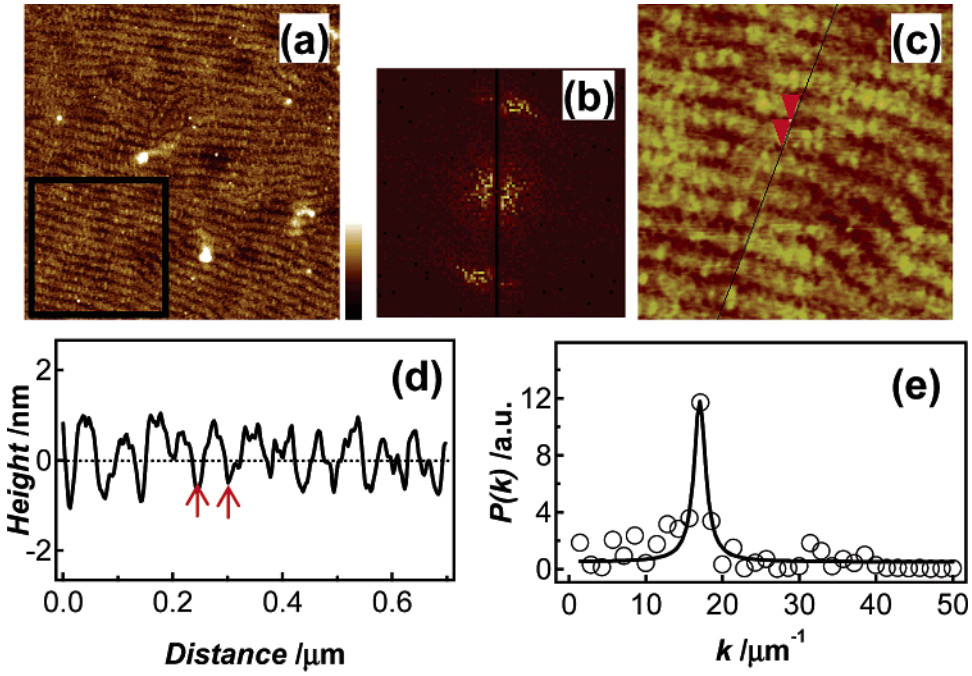

Figure 1. (a) Tapping-mode AFM height image of a $M_n = 12.9$ kg·mol^{-1} PLLA LB film prepared in the LC region at $\Pi = 4.0$ mN·m^{-1}. The scan size is 2×2 μm^2, and the z range is 5 nm. (b) A 2D Fourier transform reflects the periodicity of the lamellar patterns. (c) A section of the original AFM image (box in a) is enlarged for a line scan analysis (d) and a 2D FFT (e). The line scan analysis reveals that the surface dimension of the lamellae is around 56 nm. The power spectrum (circles in e), $P(k)$, calculated from radial averages of the squared amplitudes is fit with a Lorentzian function (solid line in e) to obtain a periodicity of 58.7 ± 0.7 nm.

engineering and drug delivery.[17,18] In particular, crystallinity represents a fundamental material variable for controlling the surface morphology of poly(L-lactic acid) (PLLA) substrates.[19,20] PLLA substrates with different degrees of crystallinity can be obtained by annealing spin-coated films at different temperatures. Park and Griffith-Cima[19] suggested that cells proliferate more slowly on crystalline regions than on amorphous regions. Washburn et al.[20] found that the rate of cell proliferation decreases with increasing surface roughness. Both results are consistent given the fact that a film's surface roughness generally increases as crystals form. However, it is still not clear whether the rate of cell proliferation is controlled by crystallinity, surface roughness, or both factors. In this study, we use the LB technique to prepare PLLA substrates with high crystallinity but relatively low surface roughness. These films may prove useful for exploring the effects of crystallinity and/or surface roughness on cell proliferation.

Bulk PLLA crystallization studies show that PLLA forms left-handed 10_3 helices with a pseudo-orthorhombic unit cell possessing dimensions of $a = 1.07$, $b = 0.645$, and $c = 2.78$ nm.[21,22] Previous studies of PLLA Langmuir films suggest that PLLA forms 10_3 helices in solution before spreading onto the water subphase.[23−25] Further compression into a solidlike state at the air/water (A/W) interface does not alter the helical conformation. Our previous results show that PLLA Langmuir films exhibit a liquid expanded to condensed (LE/LC) phase transition in the monolayer region.[26] PLLA molecules are ordered during the LE/LC phase transition, giving rise to highly ordered lamellae in LB films prepared from the LC region. In this paper, nanoscale surface patterns formed in the LC state of PLLA are explored.

Experimental Section

Materials. The following should be noted: "Certain commercial materials and instruments are identified in this paper to adequately specify the experimental procedure. In no case does such identification imply recommendation or endorsement by the National Institute of Standards and Technology, nor does it imply that materials or equipments identified are necessarily the best available for the purposes". PLLA with various molar masses and poly(*tert*-butyl acrylate) (PtBA) were obtained from Polymer Source, Inc., and were used without further purification. The number average molar masses (M_n) of PLLA samples were [with polydispersity indices (M_w/M_n) in parentheses]: $M_n = 7.9$ (1.27), 12.9 (1.24), 16.8 (1.30), 24.6 (1.33), and 40.4 (1.35) kg·mol^{-1}. For PtBA, $M_n = 23.8$ kg·mol^{-1} and $M_w/M_n = 1.08$. Silicon substrates [EnCompass Materials Group, Ltd., Dopant: Phosphorus, Type N, Orientation (1,0,0)] were used to prepare PLLA LB films for AFM studies. Glass slides with one surface covered by 1 nm of chromium and 50 nm of gold (EMF Corporation) were used to prepare LB films for RAIRS studies. Detailed procedures for cleaning and hydrophobizing the silicon and gold substrates are described in the Supporting Information.

LB Film Preparation. Ultrathin LB films were obtained using a commercial LB trough (KSV 2000, KSV Instruments, Inc.) by Y-type deposition. The temperature of the subphase was maintained by circulating water through the base of the trough. Surface pressure−area per monomer ($\Pi - A$) isotherm studies used to determine transfer Π values are described in the Supporting Information (Figures S1 and S2). During deposition, the compression rate for approaching the target Π was 10 mm·min^{-1}, as was the maximum forward and reverse rate of the barriers during the dipping process to maintain a constant target Π. The dipping rates for all films prepared in this study were 10 mm·min^{-1} for both the up- and downstrokes. One dipping cycle (including one up- and one downstroke) was used to

(17) Langer, R.; Tirrell, D. A. *Nature* **2004**, *428*, 487−492.
(18) Allen, D.; Westerblad, H. *Science* **2004**, *305*, 1112−1113.
(19) Park, A.; Griffith-Cima, L. G. *J. Biomed. Mater. Res.* **1996**, *31*, 117−130.
(20) Washburn, N. R.; Yamada, K. M.; Simon, C. G.; Kennedy, S. B.; Amis, E. J. *Biomaterials* **2004**, *25*, 1215−1224.
(21) De Santis, P.; Kovacs, A. J. *Biopolymers* **1968**, *6*, 299−306.
(22) Okihara, T.; Tsuji, M.; Kawaguchi, A.; Katayama, K. I.; Tsuju, H.; Hyon, S. H.; Ikada, Y. *J. Macromol. Sci., Phys.* **1991**, *B30*, 119−140.
(23) Bourque, H.; Laurin, I.; Pezolet, M.; Klass, J. M.; Lennox, R. B.; Brown, G. R. *Langmuir* **2001**, *17*, 5842−5849.
(24) Klass, J. M.; Lennox, R. B.; Brown, G. R.; Bourque, H.; Pezolet, M. *Langmuir* **2003**, *19*, 333−340.
(25) Pelletier, I.; Pezolet, M. *Macromolecules* **2004**, *37*, 4967−4973.
(26) Ni, S. L.; Lee, W. J.; Li, B. B.; Esker, A. R. *Langmuir* **2006**, *22*, 3672−3677.

prepare PLLA LB films of various molar masses on silicon substrates for AFM studies at $\Pi = 4.0$ mN·m^{-1} for $M_n = 12.9$, 16.8, 24.6, and 40.4 kg·mol^{-1}, and 6.0 mN·m^{-1} for $M_n = 7.9$ kg·mol^{-1} with transfer ratios approaching 1.0. For X-ray reflectivity measurements, PLLA bilayers were deposited at $\Pi = 7.0$ mN·m^{-1} and PtBA was transferred at $\Pi = 19.0$ mN·m^{-1}. In both cases, the transfer ratios were ~1.0 for all up- and downstrokes. For the case of reflection absorption infrared spectroscopy (RAIRS) experiments, PLLA multilayers were also transferred at $\Pi = 7.0$ mN·m^{-1}. Additional deposition information is also provided in the Supporting Information.

LB Film Characterization. Atomic force microscopy (AFM) images were obtained in the tapping mode with a Digital Instruments Dimension 3000 Scope and a Nanoscope IIIa controller using etched single-crystal silicon tips. Images [5 × 5 μm^2 or 2 × 2 μm^2] were captured at a set-point ratio of ca. 0.6. Smaller images presented were cut from the original image using ACDSee. X-ray reflectivity was performed at the NIST Center for Neutron Research using Cu Kα radiation with a wavelength of 1.542 Å on a Bruker AXS-D8 Advance diffractometer. RAIRS was performed using a Bruker IFS 66v/S spectrometer using *p*-polarized light at an incident angle of 86° and a liquid-nitrogen cooled MCT (mercury−cadmium−telluride) detector. Clean gold substrates served as background references. Each spectrum was collected using a minimum resolution of 2 cm^{-1} and represents an average of 1000 scans.

Results and Discussion

Figure 1a shows well-ordered lamellar features obtained for a $M_n = 12.9$ kg·mol^{-1} PLLA LB film via AFM.[26] The lamellar features are parallel to the LB film deposition direction, as shown in the Supporting Information (Figures S3−S5). The orientation of the lamellae suggests that the shape persistent features behave like rigid rod polymers (a detailed discussion is provided in the Supporting Information).[27−31] A 2D Fourier transform of the 2 × 2 μm^2 AFM image in Figure 1a shows an anisotropic periodic structure with a length scale around 56 nm (Figure 1b). To clearly examine the lamellae, a 0.7 × 0.7 μm^2 portion (Figure 1c) is cut from the original 2 × 2 μm^2 AFM image (box in Figure 1a) and is subjected to a line scan analysis and a subsequent 2D fast Fourier transform (FFT). The line scan analysis shows that the surface dimension of the bright lamellar features (Figure 1d) is around 55.7 ± 0.5 nm. A radial average of the squared FFT amplitude is used to obtain the power spectrum, $P(k)$, which is fit with a Lorentzian function (Figure 1e). The power spectrum exhibits a maximum at 17.0 ± 0.2 μm^{-1}, indicating that the periodicity is 58.7 ± 0.7 nm.[32]

The estimates of the lamellar dimension obtained from Figure 1 are interesting because a $M_n = 12.9$ kg·mol^{-1} PLLA molecule contains approximately 180 repeating units, or a maximum of 18 10_3-helical repeating units. According to the pseudo-orthorhombic unit cell,[22] each 10_3 helix has a linear dimension of 2.78 nm. Hence a single chain of 12.9 kg·mol^{-1} PLLA will be 50 nm long if the entire chain is in a perfect 10_3-helical conformation. The similarity between the calculated chain length and the lamellar dimension from AFM images suggests that individual PLLA chains exist as 10_3 helices that persist over nearly the entire length of the chain with disordered chain ends. This hypothesis is supported by molar mass scaling of the lamellar dimensions. Lamellar patterns are observed for all AFM images as seen for representative AFM images in Figure 2a−d. Lamellar spacings are determined following the same analysis scheme used in Figure 1. A linear relationship is observed in Figure 2e between lamellar spacing and the number average degree of polymerization (M_n/M_0, where M_0 is the molar mass of the repeating unit). The slope of the line in Figure 2e is 0.273 ± 0.007 nm, which is in excellent agreement with the expected value of 0.278 nm·monomer^{-1} for PLLA 10_3 helices.[22] Based on this analysis, the contrast in the AFM images presumably arises from helical segments (bright region) with amorphous chain ends (dark region), yielding smooth PLLA LB-films with lamellar patterns. The root-mean-squared (rms) surface roughness value for Figure 1c is ~0.3 nm.

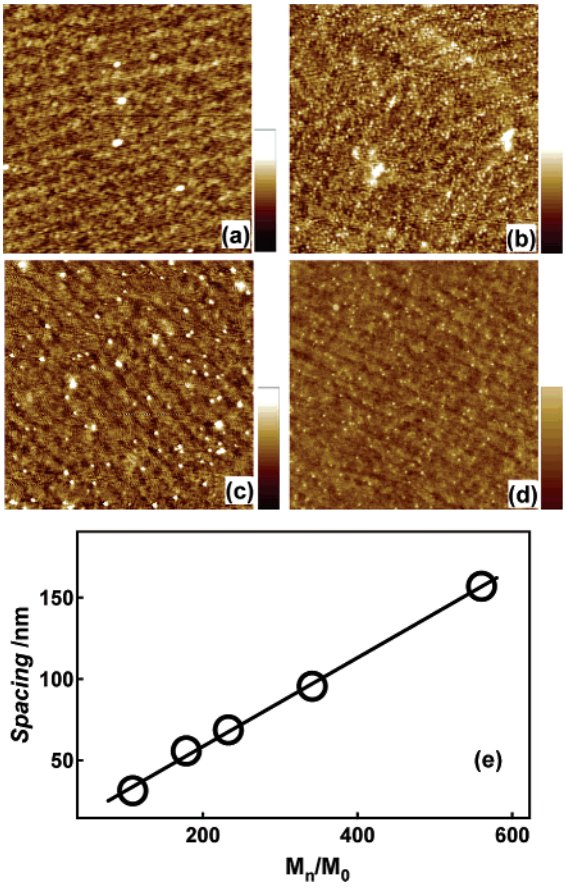

Figure 2. Tapping mode AFM height images of variable M_n PLLA LB films prepared in the LC monolayer regions: (a) 7.9 (1 × 1 μm^2) at $\Pi = 6.0$ mN·m^{-1}, (b) 16.8 (2 × 2 μm^2), (c) 24.6 (2 × 2 μm^2), and (d) 40.4 (2.5 × 2.5 μm^2) kg·mol^{-1} at $\Pi = 4.0$ mN·m^{-1}. The *z* range for all images is 5 nm. (e) A plot of lamellar spacing versus the number average degree of polymerization. One standard deviation error bars for individual data points are smaller than the symbol size and are not displayed. The slope of the best linear fit (solid line) is 0.273 ± 0.007 nm.

Moreover, AFM results suggest 10_3 helices lie flat in the plane of the film. To check this feature, X-ray reflectivity measurements were performed to measure the thickness of a PLLA monolayer. Because of the difficulty of quantitatively preparing uniform PLLA LB films thicker than a bilayer and the challenge of unambiguously measuring the thickness of a film <1 nm thick, a special film configuration was developed to produce films of suitable thickness for a model independent analysis of film thickness from X-ray reflectivity data.[33,34] To accomplish this goal, a LB multilayer film of PtBA is transferred on top of a PLLA LB bilayer on a Si wafer, to yield films with configurations of air//PtBA (variable thickness, *N* layers)//PLLA (bilayer)//Si

(27) Wegner, G. *Thin Solid Films* **1992**, *216*, 105−116.
(28) Schwiegk, S.; Vahlenkamp, T.; Xu, Y. Z.; Wegner, G. *Macromolecules* **1992**, *25*, 2513−2525.
(29) Yase, K.; Schwiegk, S.; Lieser, G.; Wegner, G. Y. *Thin Solid Films* **1992**, *210/211*, 22−25.
(30) Wang, X. Y.; Chen, Y. L.; Liu, H. G.; Jiang, J. Z. *Thin Solid Films* **2006**, *496*, 619−625.
(31) Sauer, T.; Arndt, T.; Batchelder, D.; Kalachev, A. A.; Wegner, G. *Thin Solid Films* **1990**, *187*, 357−374.
(32) Nisato, G.; Ermi, B. D.; Douglas, J. F.; Karim, A. *Macromolecules* **1999**, *32*, 2356−2364.

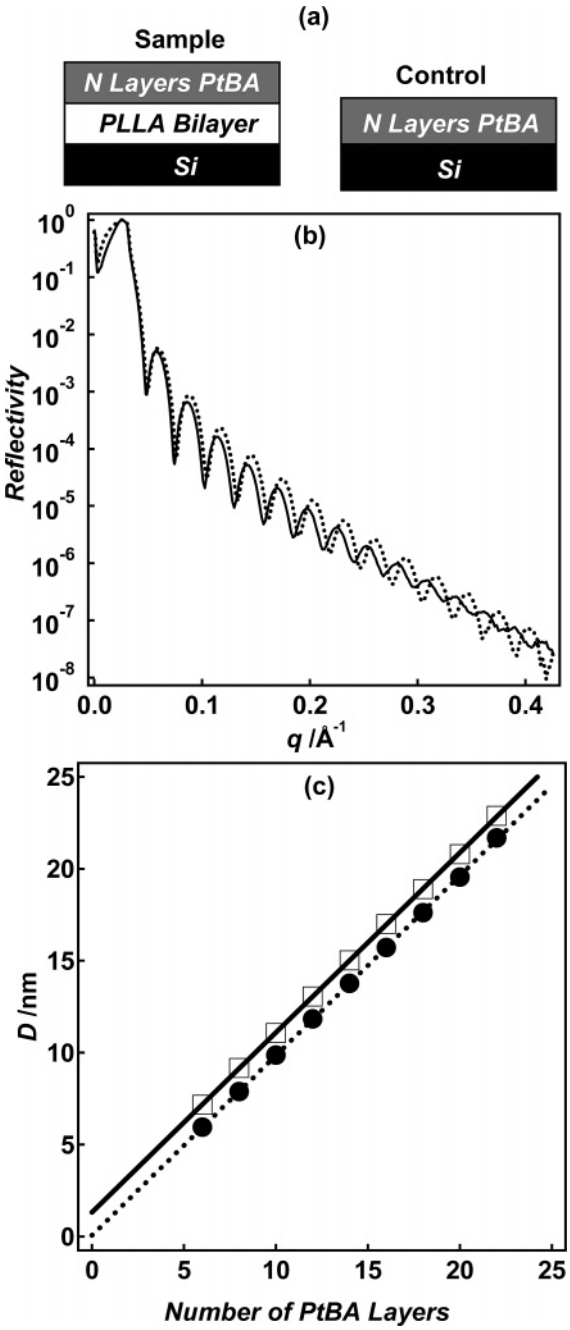

Figure 3. (a) Schematic depiction of the sample and control films, (b) representative X-ray reflectivity profiles, and (c) the dependence of the film thickness on the number of PtBA layers. The dotted curve in (b) shows the X-ray reflectivity profiles for a 22 layer PtBA film, and the solid curve corresponds to a 22 layer PtBA film on top of a PLLA bilayer. The dotted line and the filled circles in (c) represent thickness data for PtBA films, and the solid line and open squares correspond to similar data for PtBA films on PLLA bilayers.

as depicted in Figure 3a, where "//" represents a distinct interface. PtBA is chosen for the top layer because it can quantitatively form LB multilayer films with surface roughness values <1 nm.[12] *N* varies from 6 to 22, with increments of 2 layers. Figure 3b shows representative X-ray reflectivity profiles for a 22 layer PtBA control film and a sample film with 22 PtBA layers and 2 PLLA layers. X-ray reflectivity profiles for the other *N* layers of PtBA are shown in the Supporting Information (Figure S6). The X-ray reflectivity profiles have been corrected for the fraction of the incident beam subtended by the sample by subtracting background scans. Compared to pure PtBA LB films, the films

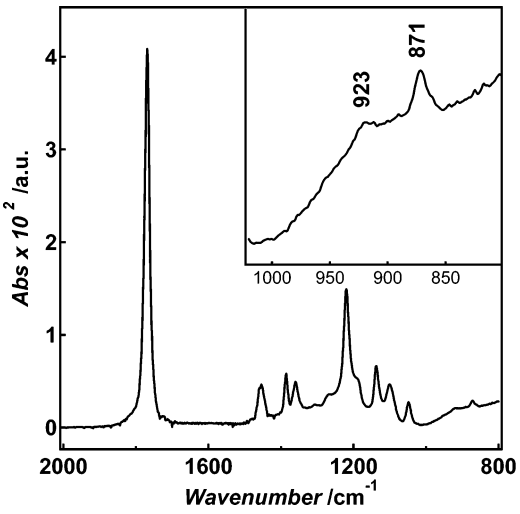

Figure 4. RAIRS spectrum of a 10 layer LB-film of 12.9 kg·mol^{-1} PLLA prepared in the LC monolayer region at $\Pi = 7.0$ mN·m^{-1}. An enlargement of the region between 1020 and 800 cm^{-1} is shown in the inset. Two characteristic bands sensitive to the 10_3 helical conformation of PLLA are observed at 923 and 871 cm^{-1}, confirming the existence of PLLA 10_3 helices in the as-prepared LB films.[37,38]

containing two PLLA layers are thicker and have rougher surfaces as indicated by roughness values of ~0.5 nm for pure PtBA and ~0.7 nm for PLLA//PtBA films (obtained by fitting the experimental reflectivity profiles as described in the Supporting Information).[35,36] The film thickness, *D*, is obtained from an analysis of the X-ray reflectivity profiles (as described in the Supporting Information)[33] and is plotted against the PtBA layer number for both pure PtBA films and PtBA//PLLA films (Figure 3c). The linear relationships confirm that PtBA is quantitatively transferred onto both hydrophobic Si and the PLLA bilayer. The identical slopes (≅0.978 ± 0.003 nm layer^{-1}) provide the thickness of a PtBA monolayer.[12] The difference in the *y* intercepts (≅ 1.24 ± 0.06 nm) provides the thickness of two PLLA layers on the basis of the film configuration. Hence, the thickness of a PLLA monolayer is determined to be 0.62 ± 0.03 nm and is consistent with the corresponding parameter of the pseudo-orthorhombic unit cell ($b = 0.645$ nm).[22] This result is consistent with the hypothesis that 10_3 helices lie flat in the plane of the film.

In addition, the existence of helices is confirmed by RAIRS studies on PLLA LB-films deposited on gold substrates. Figure 4 shows the RAIRS spectrum of a 10-layer 12.9 kg·mol^{-1} PLLA LB film prepared at $\Pi = 7.0$ mN·m^{-1}. A peak is observed at 923 cm^{-1}, which is assigned to the coupling of C−C backbone stretching with the CH_3 rocking mode and is sensitive to the 10_3-helical chain conformation of PLLA α crystals.[37,38] Another band is also observed at 871 cm^{-1} that is also sensitive to the 10_3-helical conformation.[37] The presence of these characteristic bands confirms the existence of PLLA 10_3 helices in the as-prepared PLLA LB films.

Conclusions

In summary, the PLLA monolayer thickness from X-ray reflectivity measurements, the molar mass dependence of the

(33) Thompson, C.; Saraf, R. F.; Jordan-Sweet, J. L. *Langmuir* **1997**, *13*, 7135−7140.
(34) Schaub, M.; Fakirov, C.; Schmidt, A.; Lieser, G.; Wenz, G.; Wegner, G.; Albouy, P. A.; Wu, H.; Foster, M. D.; Majrkzak, C.; Satija, S. *Macromolecules* **1995**, *28*, 1221−1228.
(35) Russell, T. P. *Mater. Sci. Rep.* **1990**, *5*, 171−271.
(36) Welp, K. A.; Co, C. C.; Wool, R. P. *J. Neutron Res.* **1999**, *8*, 37.
(37) Zhang, J. M.; Tsuji, H.; Noda, I.; Ozaki, Y. *J. Phys. Chem. B* **2004**, *108*, 11514−11520.
(38) Kister, G.; Canssanas, G.; Vert, M. *Polymer* **1998**, *39*, 267−273.

lamellar dimensions from AFM images, and the existence of the characteristic bands for PLLA 10_3 helices from RAIRS are consistent with PLLA molecules existing in a 10_3-helical conformation over nearly the entire length of a polymer chain in LB films and presumably at the A/W interface as well given previous studies by polarization modulation infrared reflection absorption spectroscopy.[23−25] It is also necessary to distinguish between the lamellar patterns in PLLA LB films and conventional ones that arise from phase separation in block copolymers[39,40] or crystallization in semicrystalline polymers.[41,42] Unlike the lamellar patterns recently observed for isotactic poly(methyl methacrylate) where the lamellae represent folded-chain crystals,[43] the lamellae formed from single molecule helices of PLLA have no chain folding. In this respect, PLLA chains act like small liquid-crystalline molecules and rigid-rod polymers. For example, Wu et al. could see individual chains near liquid crystal defects in phthalocyanine systems.[44] More recently, single molecules of conjugated copolymers[45] and conductive polymers[46] have also been observed. Here, single molecule PLLA helices form smectic lamellar patterns in LB films that also exhibit disinclinations. Further work is currently in progress to examine the crystallization kinetics of the single-chain helices in confined geometries by in situ AFM and RAIRS.

Acknowledgment. The authors thank Prof. Herve Marand (Virginia Tech) and Prof. Hyuk Yu (University of Wisconsin−Madison) for useful discussions, Mr. Steve McCartney for his training and assistance with AFM, and the National Science Foundation (CHE-0239633), the Army Research Office (W911NF-04-1-0195), and the National Research Initiative of the USDA Cooperative State Research, Education and Extension Service, Grant Number 2005-35504-16088 for financial support.

Supporting Information Available: Isotherm studies, cleaning of Si and gold substrates, LB-film deposition information, AFM images of additional LB films and Langmuir−Schaeffer films, X-ray reflectivity profiles, and fitting procedures for X-ray reflectivity profiles. This material is available free of charge via the Internet at http://pubs.acs.org.

LA060734A

(39) Folkes, M. J.; Keller, A. *J. Polym. Sci., Part B: Polym. Phys.* **1976**, *14*, 833−843.
(40) Bates, F. S. *Science* **1991**, *251*, 898−905.
(41) Keller, A. *Philos. Mag.* **1957**, *2*, 1171−1175.
(42) Fischer, E. W. *Z. Naturforsch.* **1957**, *12a*, 753−754.
(43) Kumaki, J.; Kawauchi, T.; Yashima, E. *J. Am. Chem. Soc.* **2005**, *127*, 5788−5789.
(44) Wu, J. H.; Lieser, G.; Wegner, G. *Adv. Mater.* **1996**, *8*, 151−154.
(45) Sakaguchi, H.; Matsumura, H.; Gong, H.; Abouelwafa, A. M. *Science* **2005**, *310*, 1002−1006.
(46) Bocharova, V.; Kiriy, A.; Vinzelberg, H.; Monch, I.; Stamm, M. *Angew. Chem., Int. Ed.* **2005**, *44*, 6391−6394.